

# Applications of Cellular Neural Networks for Shape from Shading Problem

Mariofanna Milanova<sup>1</sup>, Paulo E. M. Almeida<sup>2</sup>, Jun Okamoto Jr.<sup>1</sup> and Marcelo Godoy Simões<sup>1</sup>

<sup>1</sup> Department of Mechanical Engineering – Escola Politécnica – USP  
Av. Prof. Mello Moraes, 2231 - São Paulo 05508-900, SP – BRAZIL  
FAX : +55-11-813-1886  
milanova@lyra.mcca.ep.usp.br, {jokamoto, mgs}@usp.br

<sup>2</sup> Department of Research and Postgraduate / CEFET – MG  
Av. Amazonas, 7675 - Belo Horizonte 30510-000, MG – BRAZIL  
FAX : +55-31-319-5212  
paulo@dppg.cefetmg.br

**Abstract.** The Cellular Neural Networks (CNN) model consist of many parallel analog processors computing in real time. CNN is nowadays a paradigm of cellular analog programmable multidimensional processor array with distributed local logic and memory. One desirable feature is that these processors are arranged in a two dimensional grid and have only local connections. This structure can be easily translated into a VLSI implementation, where the connections between the processors are determined by a cloning template. This template describes the strength of nearest-neighbour interconnections in the network. The focus of this paper is to present one new methodology to solve Shape from Shading problem using CNN. Some practical results are presented and briefly discussed, demonstrating the successful operation of the proposed algorithm.

## 1 Introduction

The contrast between artificial and natural vision systems is due to the inherent parallelism and continuous time and signal values of the latter. In particular, the cells of the natural retina combine photo transduction and collective parallel processing for the realization of low-level image processing operations (feature extraction, motion analysis, etc.), concurrently with the acquisition of the image. Having collected spatio-temporal information from the imagery, there exist spatial representations of this information. The Cellular Neural Network paradigm is considered as a unifying model for spatio-temporal properties of the visual system [1],[2].

Many visual tasks are related to visual reconstruction and can be treated as optimization problems. Examples are shape from shading, edge detection, motion analysis, structure from motion and surface interpolation. These ill-posed, inverse problems yield a solution through minimization techniques. From Poggio [4] (see

Table 1), it can be observed that various early and intermediate level computer vision tasks are obtained by energy minimization of various functionals.

As shown by Koch [5], quadratic variational problems can be solved by linear, analog electrical or chemical networks using regularization techniques, additive models or Markov random fields (MRF) approaches. However, quadratic variational principles have limitations. The main problem is the degree of smoothness required for the unknown function that has to be recovered. For instance, the surface interpolation scheme outlined above smoothes over edges and thus fails to detect discontinuities.

**Table 1.** Problems and the Corresponding Functionals

<b>Problem</b>	<b>Regularization principle</b>
Edge detection	$\int [(Sf - i)^2 + \lambda(f_{xx})^2] dx$
Area based Optical flow	$\int [(i_x u + i_y v + i_t)^2 + \lambda(u_x^2 + u_y^2 + v_x^2 + v_y^2)] dx dy$
Contour based Optical Flow	$\int [(V \cdot N - V^N)^2 + \lambda \left( \frac{dV}{dx} \right)^2]$
Surface Reconstruction	$\int [(S \cdot f - d^2 + \lambda(f_{xx}^2 + 2f_{xy}^2 + f_{yy}^2))] dx dy$
Spatio-temporal approximation	$\int [(S \cdot f - i)^2 + \lambda(\nabla f \cdot V + ft)^2] dx dy dt$
Color	$\  I^y - Ax \ ^2 + \lambda \  Pz \ ^2$
Shape from Shading	$\int [(E - R(f, g))^2 + \lambda(f_x^2 + f_y^2 + g_x^2 + g_y^2)] dx dy$
Stereo	$\int \left\{ [\nabla^2 G^*(L(x, y) - R(x+d)x, y)]^2 + \lambda(\nabla d)^2 \right\} dx dy$
Contours	$\int E_{snake} (v(s)) ds$

Hopfield and Tank have shown that networks of nonlinear analog „neurons“ can be effective in computing the solution of optimization problems (traveling salesman problem, stereo matching problem, etc. [20]).

The focus of this paper is to present a new methodology to solve Shape from Shading problem. For that purpose, a regularization technique is used, based on Markov random fields (MRF) modeling and energy minimization via the iterated relaxation algorithm. We started from mathematical viewpoint (i.e., statistical regularization based on MRF) and mapping the algorithm onto an analog network

(CNN). Robust shape recovering is achieved by using spatio-temporal neighborhood for modeling pixel interactions.

This paper is organised as follows. In Section 2, the architecture of CNN is briefly reviewed. In Section 3, a new method for surface reconstruction is proposed. Experimental results are presented in Section 4 and section 5 concludes the paper.

## 2 Architecture of Cellular Neural Networks

Cellular Neural Networks (CNN) and the CNN universal machine (CNN-UM) were introduced in 1988 and 1992, respectively [1]-[3]. The most general definition of such networks is that they are arrays of identical dynamical systems, the cells, that are only locally connected [2]. In the original Chua and Yang model, each cell is a one-dimensional dynamic system. It is the basic unit of a CNN. Any cell is connected only to its neighbour cells, i.e. adjacent cells interact directly with each other. Cells not in the immediate neighbourhood have indirect effect because of the propagation effects of the dynamics in the network. The cell located in the position  $(i,j)$  of a two-dimensional  $M \times N$  array is denoted by  $C_{ij}$ , and its  $r$ -neighbourhood  $N^r_{ij}$  is defined by

$$N^r_{ij} = \{C_{kl} \mid \max\{|k-i|, |l-j|\} \leq r; 1 \leq k \leq M, 1 \leq l \leq N\} \tag{1}$$

where the size of the neighbourhood  $r$  is a positive integer number.

Each cell has a state  $x$ , a constant external input  $u$ , and an output  $y$ . The equivalent block diagram of a continuous time cell is shown in Figure 1.

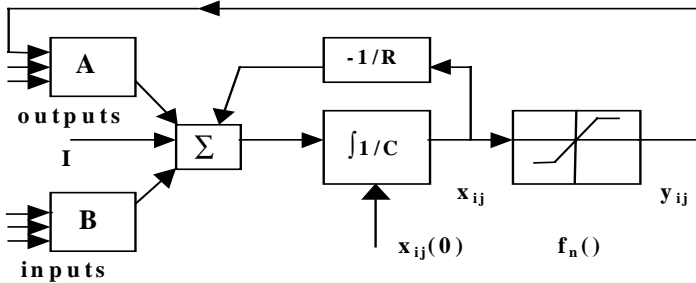


Fig. 1. Block diagram of one cell

The first-order non-linear differential equation defining the dynamics of a cellular neural network can be written as follows:

$$C \frac{\partial x_{ij}(t)}{\partial t} = -\frac{1}{R} x_{ij}(t) + \sum_{C_{kl} \in N^r_{ij}} A(i, j; k, l) y_{kl}(t) + \sum_{C_{kl} \in N^r_{ij}} B(i, j; k, l) u_{kl} + I \tag{2}$$

$$y_{ij}(t) = \frac{1}{2} \left( \left| x_{ij}(t) + 1 \right| - \left| x_{ij}(t) - 1 \right| \right)$$

where  $x_{ij}$  is the state of cell  $C_{ij}$ ,  $C$  and  $R$  conform the integration time constant of the system, and  $I$  is an independent bias constant. From [2],  $y_{ij}(t) = f(x_{ij}(t))$ , where  $f$  can be any convenient non-linear function.

The matrices  $A(\cdot)$  and  $B(\cdot)$  are known as cloning templates.  $A(\cdot)$  acts on the output of neighbouring cells and is referred to as the feedback operator.  $B(\cdot)$  in turn affects the input control and is referred to as the control operator. Of course,  $A(\cdot)$  and  $B(\cdot)$  are application dependent. A constant bias  $I$  and the cloning templates determine the transient behaviour of the cellular non-linear network. In general, the cloning templates do not have to be space invariant, they can be, but it is not a necessity. A significant feature of CNN is that it has two independent input capabilities: the generic input and the initial state of the cells. Normally they are bounded by

$$|u_{ij}(t)| \leq 1 \quad \text{and} \quad |x_{ij}(0)| \leq 1 \quad (3)$$

Similarly, if  $|f(\cdot)| \leq 1$  then  $|y_{ij}(t)| \leq 1$ .

When used as an array processing device, the CNN performs a mapping

$$\left. \begin{array}{l} x_{ij}(0) \\ u_{ij}(t) \end{array} \right\} : F \Rightarrow y_{ij}(t) \quad (4)$$

where  $F$  is a function of the cloning template  $(A, B, I)$ .

The functionality of the CNN array can be controlled by the cloning template  $A, B, I$ , where  $A$  and  $B$  are  $(2r+1) \times (2r+1)$  real matrices and  $I$  is a scalar number in two-dimensional cellular neural networks. In many applications,  $A(i,j;k,l)$  and  $B(i,j;k,l)$  are space invariant. If  $A(i,j;k,l) = A(k,l;i,j)$ , then the CNN is called symmetrical or reciprocal.

There are two main cases of CNN: continuous-time (CT-CNN) and discrete-time (DT-CNN) cellular neural networks. The equations for each cell of a DT-CNN are

$$\begin{aligned} x_{ij}^{(k)} &= \sum_{C_{kl} \in N^{r_{ij}}} A(i,j;k,l) y_{kl}^{(k)} + \sum_{C_{kl} \in N^{r_{ij}}} B(i,j;k,l) u_{kl} + I_{ij} \\ y_{ij}^{(k)} &= f(x_{ij}^{(k-1)}) \\ f(x) &= \text{sgn}(x) \end{aligned} \quad (5)$$

A special class of two-dimensional cellular neural network is described by ordinary differential equations of the form (see [2], [10]).

$$\begin{aligned} \frac{\partial x_{ij}(t)}{\partial t} &= -a_{ij} x_{ij}(t) + \sum T_{ij,kl} \text{sat}(x_{kl}(t)) + I_{ij} \\ y_{ij}(t) &= \text{sat}(x_{ij}(t)) \end{aligned} \quad (6)$$

where  $1 \leq i \leq M$ ,  $1 \leq j \leq N$ ,  $a_{ij} = 1/RC > 0$ , and  $x_{ij}$  and  $y_{ij}$  are the states and the outputs of the network, respectively, and  $\text{sat}(\cdot)$  represents the activation function.

We consider zero inputs ( $u_{ij} \equiv 0$  for all  $i$  and  $j$ ) and a constant bias vector  $I = [I_{11}, I_{12}, \dots, I_{MN}]^T$ .

Under these circumstances, we will refer to (6) as a zero-input non-symmetric cellular neural network where the  $n$  neurones are arranged in a  $M \times N$  array (with  $n = M \times N$ ) and the interconnection structure is restricted to local neighbourhoods of radius  $r$ .

System (6) is a variant of the recurrent Hopfield model with activation function  $sat(\cdot)$ . There are also several differences from the Hopfield model: 1) The Hopfield model requires that  $T$  is symmetric. We do not make this assumption for  $T$  here. 2) The Hopfield model is allowed to operate asynchronously, but the present model is required to operate in a synchronous mode. 3) In a Hopfield network used as an associative memory, the weights are computed by a Hebb rule correlating the prototype vectors to be stored, while the connections in the Cellular Neural Network are only local. For example, a CNN of the form (11) with  $M=N=9$  and  $r=3$ , has 2601 total interconnections, while a fully connected NN with  $n=81$  will have a total of 6561 interconnections.

The most popular application for CNN has been in image processing, essentially because of their analog feature and sparse connections, which are conducive to real-time processing [1], [8], [9].

A two dimensional CNN can be viewed as a parallel non-linear two-dimensional filter and have already been applied for noise removal, shape extraction, edge detection, etc.

### 3 Solving the Shape from Shading Problem by Means of CNN

#### 3.1 The Shape from Shading Problem

Shape from shading (SFS) refers to the process of reconstructing, from a unique monocular 2D image, its corresponding 3D shape. The success of SFS depends on two factors: 1) a suitable imaging model that specifies the relationship between surface shape and image brightness and 2) a good numerical algorithm for the reconstruction of shape from the given image.

In SFS research, the image model is specified through a reflectance map  $R(p,q)$ , with  $p=dz/dx$  and  $q=dz/dy$  being the partial derivatives of height  $z$  with respect to image coordinates and called the surface gradients at  $(x,y)$ . With the reflectance map determined, the SFS problem becomes one of finding the best way to reconstruct a surface  $z(x,y)$ , satisfying the image irradiance equation

$$I(x, y) = \eta \cdot n \cdot L = R(p, q) = \eta \frac{1 + pp_s + qq_s}{(1 + p^2 + q^2)^{1/2} (1 + p_s^2 + q_s^2)^{1/2}} \quad (7)$$

$$p = z_{ij} - z_{i,j+1} \quad \text{and} \quad q = z_{ij} - z_{i+1,j}$$

where  $\eta$  is called the albedo such that  $0 < \eta < 1$ , and it represents the deviation in reflectance properties due to pigmentation or markings on the surface;  $I(x,y)$  is the image intensity at position  $(x,y)$ , and  $n$  is the surface normal represented by

$$n = \frac{(-p, -q, 1)}{(1 + p^2 + q^2)^{1/2}} \quad (8)$$

$L$  is a vector representing the incident light, calculated by

$$L = \frac{(-p_s, -q_s, 1)}{(1 + p_s^2 + q_s^2)^{1/2}} \quad (9)$$

Shape from shading is precisely an inverse rendering or inverse graphics problem: given the image  $I(x,y)$ , find the surface  $S$ , the albedo  $\eta$  and the light  $L$  that satisfy equation (7).

Equation (7) (or image irradiance equation) can be viewed as a non-linear partial differential equation for the surface function  $z = z(p,q)$ . Unfortunately, thinking of it in this way is not very useful for real images. Standard methods of numerical integration of differential equations (e.g., characteristic strip method) in practice fail. These methods are inherently too sensitive to noise and boundary conditions.

An alternative formulation is to think of shape from shading as an optimization problem where one attempts to minimize the average error between intensity and irradiance on an energy function, as showed on equation (10). The optimization approach is generally more flexible for including additional constraints and is more robust to image noise and modeling errors. Typical energy functions are derived and discussed in [11],[12][13], [14], [15],[16].

$$E = \sum_i \sum_j (I(x, y) - R(p, q))^2 + \lambda \sum_i \sum_j (p^2_x + p^2_y + q^2_x + q^2_y) + \mu \sum_i \sum_j ((z_x - p)^2 + (z_y - q)^2) \quad (10)$$

Here, the first term corresponds to the intensity error, the second term is the regularization term (smoothness measure of the surface) and the third term is the integrability term.

Grimson [17] proposed interpolation schemes to obtain depth values throughout the image, that correspond to fitting a thin flexible plate through the observed data points. These interpolation schemes can be described in terms of standard regularization theory [5]. The energy function  $E(z)$  is derived from the inverse problem

$$B.z = I + n \quad (11)$$

where the data  $I$  (intensity) and the linear operator  $B$  are known,  $n$  represents noise process, and  $z$  has to be computed by

$$E(z) = |Bz - I|^2 + \alpha |Sz|^2 \quad (12)$$

In the above equation, the first term gives a measure of the distance of the solution to the data and the second term corresponds to the regularization needed to make the problem well posed.  $S$  is a linear operator associated with a membrane plate,

depending on the kind of smoothing desired and  $\alpha$  is a regularization parameter.  $B$  is a diagonal matrix with elements equal to 1 at those locations where the depth is known and 0 at all others.

$E(z)$  can be reformulated as

$$E(V) = \frac{1}{2} \sum_{ij} T_{ij} V_i V_j + \sum_i V_i I_i \tag{13}$$

by identifying the matrix  $T$  with  $2(B^T B + \alpha S^T S)$ ,  $V$  with  $z$ ,  $I$  with  $-2B^T z$  and dropping the constant term  $z^T z$ .

For the case of quadratic regularization principles,  $E(V)$  is positive definite quadratic, and therefore the system will always converge to the unique energy minimum. However, the quadratic smoothness term uniformly suppresses changes in surface shape, irrespective of changes in intensities.

Regarding the use of neural networks in shape from shading, we are aware of previous work [18], [19]. According to Yu and Tsai [12], we can use neural network techniques to solve many problems which have already been solved by the relaxation process.

A number of researchers have used the optimization capability of the Hopfield model for specific early-vision optimization problems [6],[7]. Hopfield's idea was to solve combinatorial optimization problems by allowing the binary variable to vary continuously between 0 and 1 and to introduce terms in the energy function that forced the final solution to one of the corners of the hypercube  $[0,1]^N$ . Briefly, let the output variable  $y_i(t)$  for neuron  $i$  have the range  $0 < y_i(t) < 1$  and be a continuous and monotonic increasing function of the internal state variable  $x_i(t)$  of the neuron  $i$ :  $y_i = f(x_i)$ . The output is then given as (with a sigmoid-like function):

$$y_i = \frac{1}{2} \left( 1 + \tanh \frac{x_i}{x_0} \right) = \frac{1}{1 + e^{-2x_i/x_0}} \tag{14}$$

where  $x_0$  determines the steepness of the gain function.

Hopfield interprets the expression (13) as the Lyapunov function of the network. As shown by Bose and Liang [21], CNN is an analog Hopfield network in which the connections are limited to units in local neighborhood of individual units with bi-directional signal paths.

The dynamics of the CNN are described by the system of non-linear ordinary differential equations showed on equation (6) and by an associated computation energy function (called the Lyapunov function) which is minimized during the computation process. The resulting changing equation that determines the rate of change  $x_{ij}$  is

$$C_{ij} \frac{\partial x_{ij}(t)}{\partial t} = -\frac{x_{ij}(t)}{R_i} + \sum T_{ij,kl} y_{ij}(t) + I_{ij} \tag{15}$$

where  $y_{ij}(t) = f(x_{ij}(t))$ .

The sign-type non-linearity showed in (6) is replaced by a sigmoidal non-linearity. In this case, the system becomes a continuously valued dynamical system where gradients are well defined and classical optimization algorithms can be applied.

The Lyapunov function,  $E(t)$ , of the CNN is given by

$$E(t) = -\frac{1}{2} \sum_{(i,j)} \sum_{(k,l)} T_{ij,kl} y_{ij}(t) y_{kl}(t) + \frac{1}{2R_x} \sum_{(i,j)} y_{ij}(t)^2 - \sum_{(i,j)} I y_{ij}(t) \quad (16)$$

By using an appropriately defined energy function, stability of the CNN can be proved in the same way as an analog or continuous Hopfield network. Hopfield and Tank [20] investigated the analogy between finding a solution to a given optimization problem and setting an appropriate Lyapunov function corresponding to the additive neural model.

The analog network has two advantages. First, the function  $E$  is Lyapunov, while for a digital network it is not. Second, deeper minima of energy have generally larger basins of attraction. A randomly selected starting state has a higher probability of falling inside the basins of attraction of a deeper minimum.

### 3.2 A New Algorithm for Shape from Shading

Here we propose another method for surface reconstruction, based on the interactions between neighborhood pixels provided by the CNN and MRF paradigms. Since SFS is an intensity-driven process, the random field of intensity in small area is assumed to have MRF properties, i.e., a Gibbs distribution and a neighborhood structure. The spatio-temporal neighborhood of the pixel (or site) is given as in CNN structure.

The raw observation is at pixel level (site or node), where  $s=(i,j)$  is given by changes in the intensity function (image irradiance equation) by the function

$$o_s = I(i,j) - R(i,j) \quad (17)$$

According to Geman [22], Koch [5] and Luthon [9], one way to calculate  $Z$  and observe is to minimize an energy or cost function  $E$  consisting of two terms

$$E = E_a(z) + E_b(z) \quad (18)$$

The model energy  $E_a(z)$ , embedding a priori modeling of spatio-temporal interactions between sites, is a regularization term similar to smoothness constraints classically used to solve ill-posed problems. The attachment energy  $E_b(z)$  is the intensity error.

The energy function can be rewritten as

$$E = \sum_{i,j} \left[ k_a (z_{ij} - z_{i+1,j})^2 + k_a (z_{ij} - z_{i,j+1})^2 + k_a (z_{ij} - z_{i-1,j})^2 + k_a (z_{ij} - z_{i,j-1})^2 + k_b |I_{ij} - R_{ij}| \right] \quad (19)$$

The minimum energy may be computed using either stochastic relaxation algorithms, like simulated annealing [22], or deterministic algorithms, such as iterated conditional models (ICM) [23]. Here, the iterative method ICM is used.



The minimum of  $E$  with respect to all  $z_{ij}$  corresponds to the null partial derivatives

$$\forall_{ij} \frac{\partial E}{\partial z_{ij}} = 0 \Leftrightarrow k_a \nabla^2 z_{ij} - k_b |I_{ij} - R_{ij}| = 0 \quad (20)$$

where

$$\nabla^2 z_{ij} = 4z_{ij} - z_{i+1,j} - z_{i-1,j} - z_{i,j+1} - z_{i,j-1} \quad (21)$$

The resulting differential equation that determines the rate of change  $z_{ij}$  is

$$C \frac{\partial z_{ij}}{\partial t} = k_a \nabla^2 z_{ij} - k_b |I_{ij} - R_{ij}| \quad (22)$$

ICM relaxation runs over field  $z$ , that is scanned pixel by pixel. At each node, a local decision is taken

$$z_{ij}^{(k+1)} = k_a (4z_{ij}^{(k)} - z_{i+1,j}^{(k)} - z_{i-1,j}^{(k)} - z_{i,j+1}^{(k)} - z_{i,j-1}^{(k)}) + k_b |I_{ij} - R_{ij}^{(k)}| \quad (23)$$

This relaxation iterates until convergence is achieved at each one of the neighborhood systems defined in the field  $z$ . A relative energy decrease criterion  $\Delta E / E < \varepsilon$  is used to determine a convergent state.

## 4 Experimental Results

To verify and to demonstrate the correctness of the approach just proposed, the algorithm has been applied to some typical images in the area of image processing to perform SFS. The CNN architecture was simulated by means of the ICM relaxation algorithm above described. This algorithm iteratively increases the consistency among the states and constraints on the nodes, so that a better state, i.e., a less energetic state, can be reached at each iteration. When the algorithm converges, this means that a minimum of the correspondent energy function was found, and actual values for image depth were obtained.

For purposes of comparing the results obtained here and others in the literature, some images found on previously published papers were used. They are gray scale images with intensity values ranging from 0 to 255, and sizes varying around 300x300 pixels. First, a semispherical object illuminated from the view point is used. Figure 2 shows the original image on the left and the corresponding depth map obtained by our algorithm on the right. After, a mannequin face image is shown in figure 3. The average number of steps needed to make the relaxation algorithm to converge was found to be between 3 and 4 iteration steps.

In these experiments, the light source direction was estimated by using the techniques shown in [16]. In effect, our algorithm is very robust with respect to imprecision on the values of light source direction. It allows some range of variation in these values without reproducing significant variations on the calculated depth values. This feature can be evaluated by the experiment showed on figure 4.

As can be regarded in the figures, the algorithm has reached quite good results. In fact, the results are very close to those showed in [15]. Nevertheless, our algorithm is essentially parallel and very affordable to hardware implementation. These characteristics are the most important contribution of this work, because they allow SFS to be performed in real-time, when implemented on adequate massively parallel machines or analog VLSI dedicated circuits.

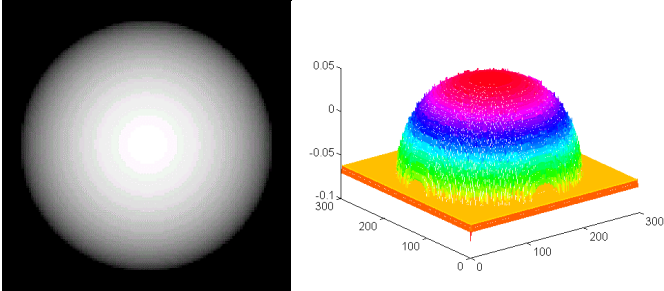


**Fig. 2.** A semispherical object and its 3D shape (input image on the left, results on the right)

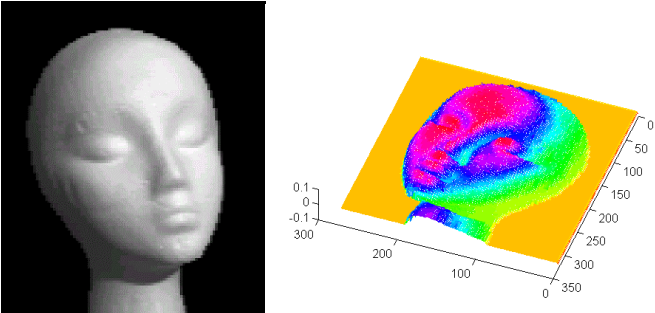


**Fig. 3.** A mannequin face and its 3D shape (input image on the left, results on the right)

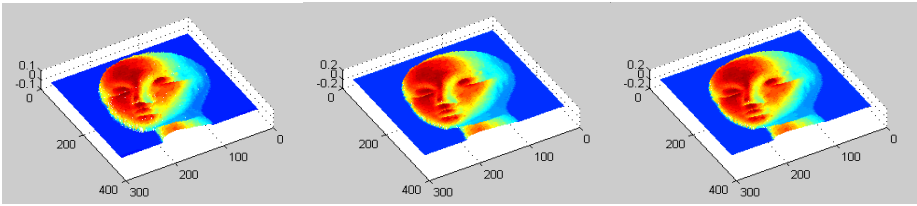


**Fig. 4.** Demonstration of the robustness of the algorithm proposed with respect to variations on the light source direction values. (a) Depth map of the mannequin face (figure 3, on the left), with  $P = Q = 1.0$ ; (b) Idem, with  $P = 1.0$ ,  $Q = 0.0$ ; (c) Idem, with  $P = 0.0$ ,  $Q = 1.0$ .

## 5 Conclusions

Some considerations about the common nature of various problems in early vision were made, concerning an optimization approach and finding a minima of an energy (Lyapunov) function of a representation model. The CNN architecture was described and found to be very suitable to perform such an optimization process, based on its intrinsic properties of evolution to a global minimal energy state.

The SFS problem was described, in terms of the variables involved and possible approaches to its solution. It was derived an energy function whose minimum value corresponds to the solution of the SFS problem, based on the concepts of spatial neighborhood and MRF. It was also showed that a CNN architecture is very affordable to implement such regularization techniques, because of the local nature of the interconnections between its neurons.

Finally, some experimental results of the algorithm proposed were showed and could be compared with others found on the literature. It can be seen that the results obtained here are similar to the old ones, but the new approach is very affordable to parallelism and analog VLSI implementation, allowing the SFS solution to be performed in real-time, if adequately implemented.

## Acknowledgements

The research reported in this article was supported by FINEP, by means of the Artificial Intelligence Net at RECOPE project, and FAPESP.

## References

1. Chua, L.O. and Yang, L. "Cellular Neural Networks: Theory and Applications", *IEEE Trans. on Circuits and Systems, (CAS)*, Vol.35 (1988), 1257-1290
2. Chua, L.O. and Roska, T. „The CNN Paradigm. *IEEE Transactions on Circuits and Systems (Part I)*“, CAS-40, 3 (1993), 147-156
3. Roska, T. and Vandewalle, J. *Cellular Neural Networks*. (John Wiley&Sons), (1993)
4. Poggio, T., Torre, V. and Koch, C. „Computational Vision and Regularisation Theory“, *Nature*, Vol. 317 (1985), 314-319
5. Koch, C., Marroquin, J. and Yuille, A. „Analog Neural Networks in Early Vision“, *Proc. Natl. Acad. Sci. USA*, Vol. 83 (1986), 4263-4267
6. Wechsler, H. *Computer Vision*, Academic Press, Inc, (1990)
7. Pajares, G., Cruz, J. and Aranda, J. „Relaxation by Hopfield Network in Stereo Image Matching“, *Pattern Recognition*, Vol. 31, No 5 (1998), 561-574
8. Radvanti A. “Structural Analysis of Stereograms for CNN Depth Detection“, *IEEE Trans. Circuits Syst. I*, Vol. 46 (1999), 239-252
9. Lithon, F. and Dragomirescu, D.“A Cellular Analog Network for MRF-Based Motion Detection“, *IEEE Trans. Circuits Syst. I*, Vol 46 (1999), 281-293
- 10.Liu, D. and Michel,A. „Sparsely Interconnected Neural Networks for Associative Memories with Applications to Cellular Neural Networks“. *IEEE Transactions on Circuits and Systems Part II Analog and Digital Signal Processing*, Vol. 41, No. 4 (1994), 295-307
- 11.Horn, B.K.P. „Obtaining Shape from Shading Information“. In *The Psychology of Computer Vision*, Winston, P.H., (Ed.). New York, McGraw-Hill, (1975), 115-155
12. Yu, S.S. and Tsai, W.H. „Relaxation by the Hopfield Neural Network“, *Pattern Recognition* , No. 25(2), (1992), 197-209
- 13.Horn, B.K.P. „Local Shading Analysis“, *IEEE Trans. Pattern Anal. Machine Intelligence*, Vol. PAMI-16, No. 2 (Mar 1984), 170-184
- 14.Pentland, A.P., „Linear Shape from Shading“, *Int. J. Comput. Vision*, Vol. 4 (1990), 153-162
- 15.Tsai, P.S. and Shah, M. „Shape from Shading using Linear Approximation“, *Research Report*, University of Central Florida, (1995)
- 16.Zheng, Q. and Chellapa, R. „Estimation of Illuminant Direction, Albedo, and Shape from Shading“, *IEEE Trans. Pattern Anal. Machine Intelligence*, Vol. 13, No. 7 (Jul 1991), 680-702

17. Grimson, W.E.L. *From Images to Surfaces: A Computational Study of the Human Early Visual System*, MIT Press, Cambridge, MA, (1981)
18. Lehky and Sejnowski. „Network Model of Shape from Shading: Neural Function Arises from both Receptive and Projective Fields“, *Nature*, Vol. 333 (Jun 1988), 452-454
19. Wei, G. and Hirzinger, G. „Learning Shape from Shading by a Multilayer Network“, *IEEE Trans. On Neural Networks*, Vol. 7, No. 4 (Jul 1996), 985-995
20. Hopfield, J. and Tank, D. „Neural Computation of Decisions in Optimization Problems“, *Biological Cybernetics*, Vol.52 (1985), 141-152
21. Bose, N.K. and Liang, P. *Neural Network Fundamentals with Graphs, Algorithms and Applications* , McGraw-Hill Series in Electrical and Computer Engineering, (1996)
22. Geman, S. and Geman, D. „Stochastic Relaxation, Gibbs Distributions, and the Bayesian Restoration of Images“, *IEEE Trans. Patter Anal. Machine Intelligence*, Vol. PAMI-6, No. 6 (Nov 1984), 721-741
23. Besag, J. „On the Statistical Analysis of Dirty Pictures“, *J. R. Statist. Soc. B*, Vol. 48, No. 3 (1986), 259-302